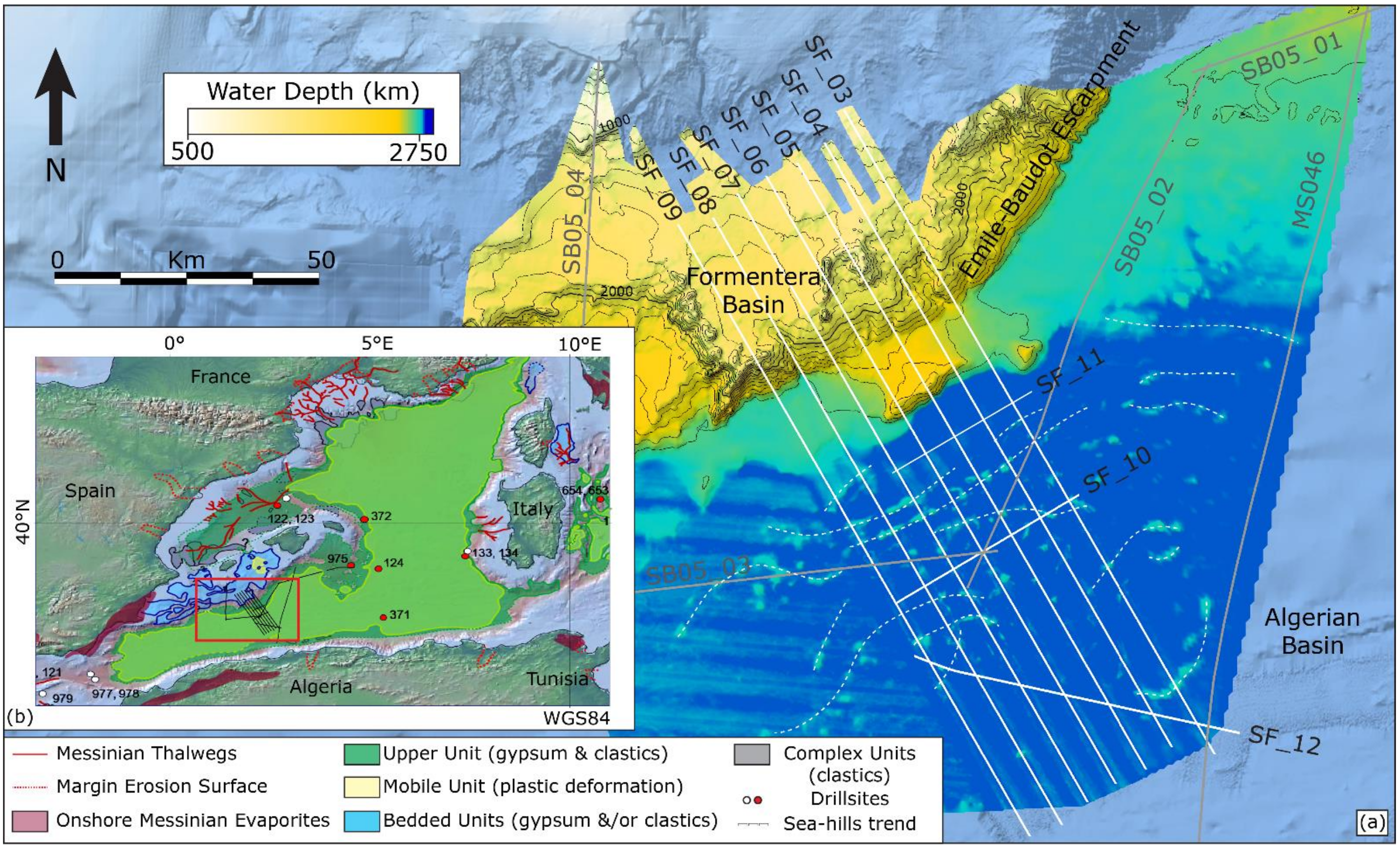

Figure 1 Study area offshore Balearic Islands, Spain. Seismic lines acquired by the National Institute of Oceanography and Applied Geophysics (OGS) are superimposed on a bathymetric map and on the relief map of the Mediterranean with DSDP and ODP drillsites (in red the ones that sampled MSC evaporites) superimposed to the present-day spatial extent of the MSC marker (Lofi, 2018). Topographic highs on the sea-bottom illustrate the presence of piercing diapiric structures. SF refers to SALTFLU lines presented in this paper, SB05 refers to survey SBAL-DEEP 2005, MS046 to profile 46 of the Mediterranean survey.

Quality Check	Processing Step	Navigation Processing
	Input Field Data	**Import raw navigation**
Cross-plot maps	**Geometry merging**	**Edit Navigation** Match FFID numbers to the corresponding shot numbers based on observer's logs
Fold distribution, Stack	**CMP Binning**	
Output difference, Stack	**1st pass Low Frequency Noise Attenuation on shot gathers** Butterworth filter 2/30dB/Oct - 110/96dB/Oct	
Time direct wave first break on near channel	**Recording delay shift statics** Shift statics of -40 ms	
Visual checking	**Resampling to 4 ms**	
Output difference, Stack	**FX Prediction Filtering (CRG)** Run 1: 0-125Hz, 20 traces x 500ms windows, amplitude threshold > 8 Run 2: 0-125Hz, 11 traces x 500ms windows, amplitude threshold > 8 Run 3: 0-3Hz, 31 traces x 1000ms windows, amplitude threshold > 1 Run 4: 0-5Hz, 11 traces x 1000ms windows, amplitude threshold > 4 Run 5: 6-12Hz, 11 traces x 500ms windows, amplitude threshold > 5	
Visual checking	**Missing shot interpolation** Sorting to Common shot gathers 1st small gap interpolation in the F-K domain using patches of 500 ms x 21 traces 2nd big gap interpolation in the F-K domain using patches of 300 ms x 125 traces	
(**Output difference, Stack**)	**Linear Radon Filtering** Passing P range -0.35 to 0.7ms/m	
(**Output difference, frequency spectrum, Stack**)	**Deghosting in FK domain** Zero padding to left and right of shot gathers Extrapolation to left and right of shot gathers Receiver-side deghost, patch 2000 ms x 21 traces, reflection coeff -0.95, Regularization 0.05 Shot-side deghost, patch 1400 ms x 240 traces, reflection coeff -0.95, Regularization 0.1	**Stacking velocity analysis** 500m CMP interval for every line
Visual checking, frequency spectrum	**Signature Estimation** Align water bottom trim corrections base on max cross-correlation peak of traces Stack	
Visual checking, frequency spectrum	**Designature operator estimation** Design matching filter between water-bottom derived signature and a targeted band limited Zero-phase Ormsby wavelet 4-8-40-120	
Output difference, Stack	**Designature Application**	
Output difference, Stack	**Low-Frequency attenuation** Ormsby low-cut filter 3-7 Hz	
Visual, Frequency spectrum	**Inverse Q correction (phase)** Q =120 below seabed, reference frequency = 50 Hz	
Residual move-out, stack	**Isotropic Pre-Stack Time Migration, then velocity refining every 250 CDP (~1.5km)** Offset regularization	
Visual	**Radon Demultiple Model** Parabolic radon transform from -200ms to 500ms (reference offset= 2500m) with an AGC wrap of 500ms Left mute (Decreasing from 100 to 30 ms depending on iterations)	
Output difference, Stack	**Multiple substraction** Data - Radon Model	
Output difference, Stack	**10 CDP (~50m), Automated residual velocity analysis** Auto-picking +- 10% velocity, every 25 ms Pick smoothing (51 CDPs)	- OUT: Pre-migration final demultiple data - OUT: Stack & Migration RMS velocity
Visual, Frequency spectrum	**Inverse Q correction (amplitude)** Q =120 below seabed, reference frequency = 50 Hz	
Stack	**Stack** Angle mute 48deg Stack Waterbottom mute	- Processed Migration stacks

Figure 2 Time domain reprocessing sequence and parameters applied to the SALTFLU dataset

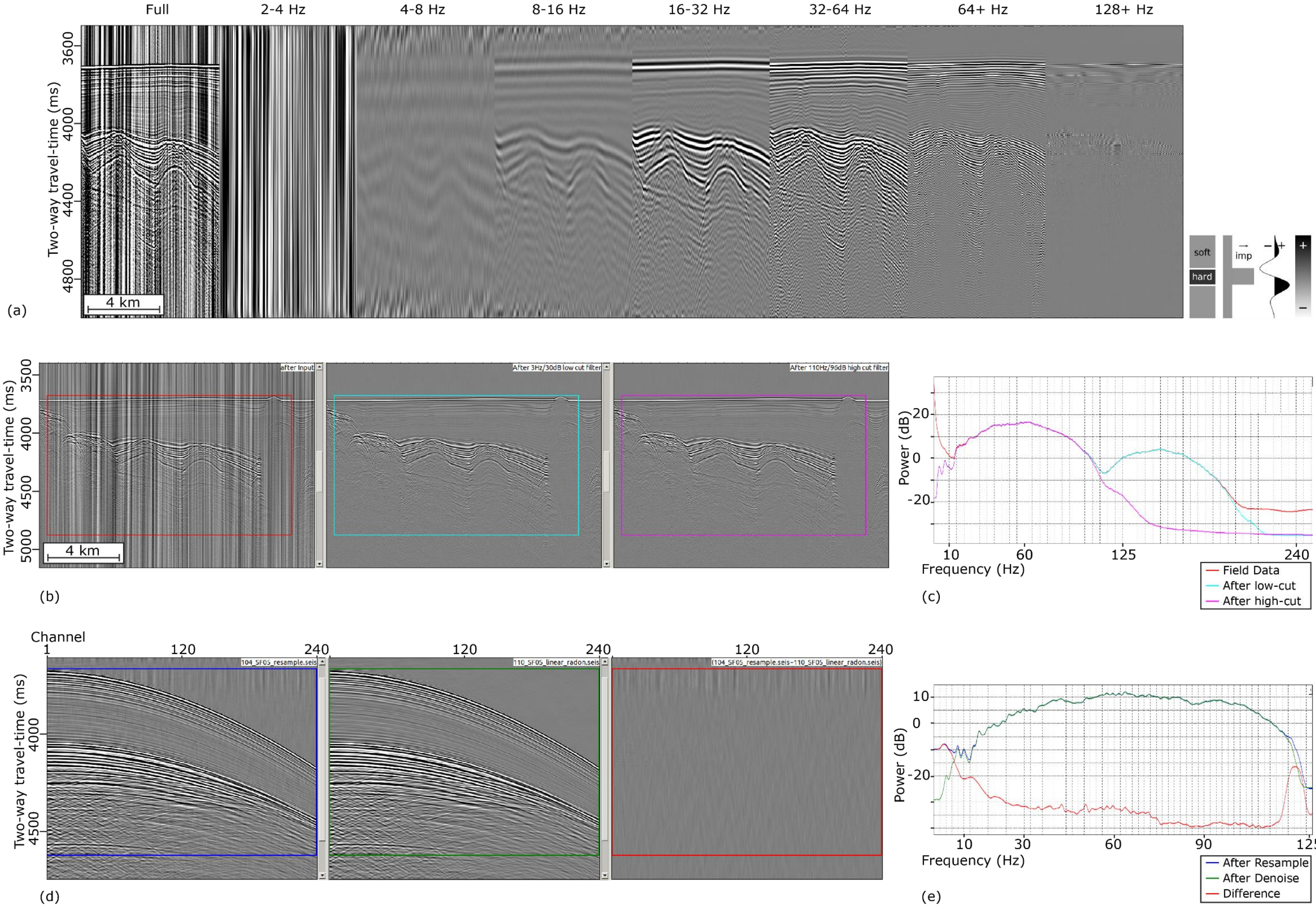
Full
2-4 Hz
4-8 Hz
8-16 Hz
16-32 Hz
32-64 Hz
64+ Hz
128+ Hz
Two-way travel-time (ms)
3600
4000
4400
4800
4 km
(a)
soft
hard
imp
+
−
after Input
After 3Hz/30dB low cut filter
After 110Hz/96dB high cut filter
3500
4000
4500
5000
(b)
Power (dB)
20
0
-20
10
60
125
240
Frequency (Hz)
Field Data
After low-cut
After high-cut
(c)
Channel
1
120
240
104_SF05_resample.seis
110_SF05_linear_radon.seis
(104_SF05_resample.seis-110_SF05_linear_radon.seis)
(d)
10
0
-20
30
90
After Resample
After Denoise
Difference
(e)

Figure 3 Seismic sections of part of the SF05 line illustrating the results at different steps of the noise attenuation stage (a) Frequency panels at different octaves of raw field data; (b) Input near-trace-plot (left), outputs after low-cut filter (middle) and high-cut filter (right); (c) Frequency spectra corresponding to (b); (d) Input shot gather after resampling to 4 ms (left) versus after linear low-frequency noise removal steps (middle), and difference panel between the two (right); (e) Frequency spectra corresponding to (d).

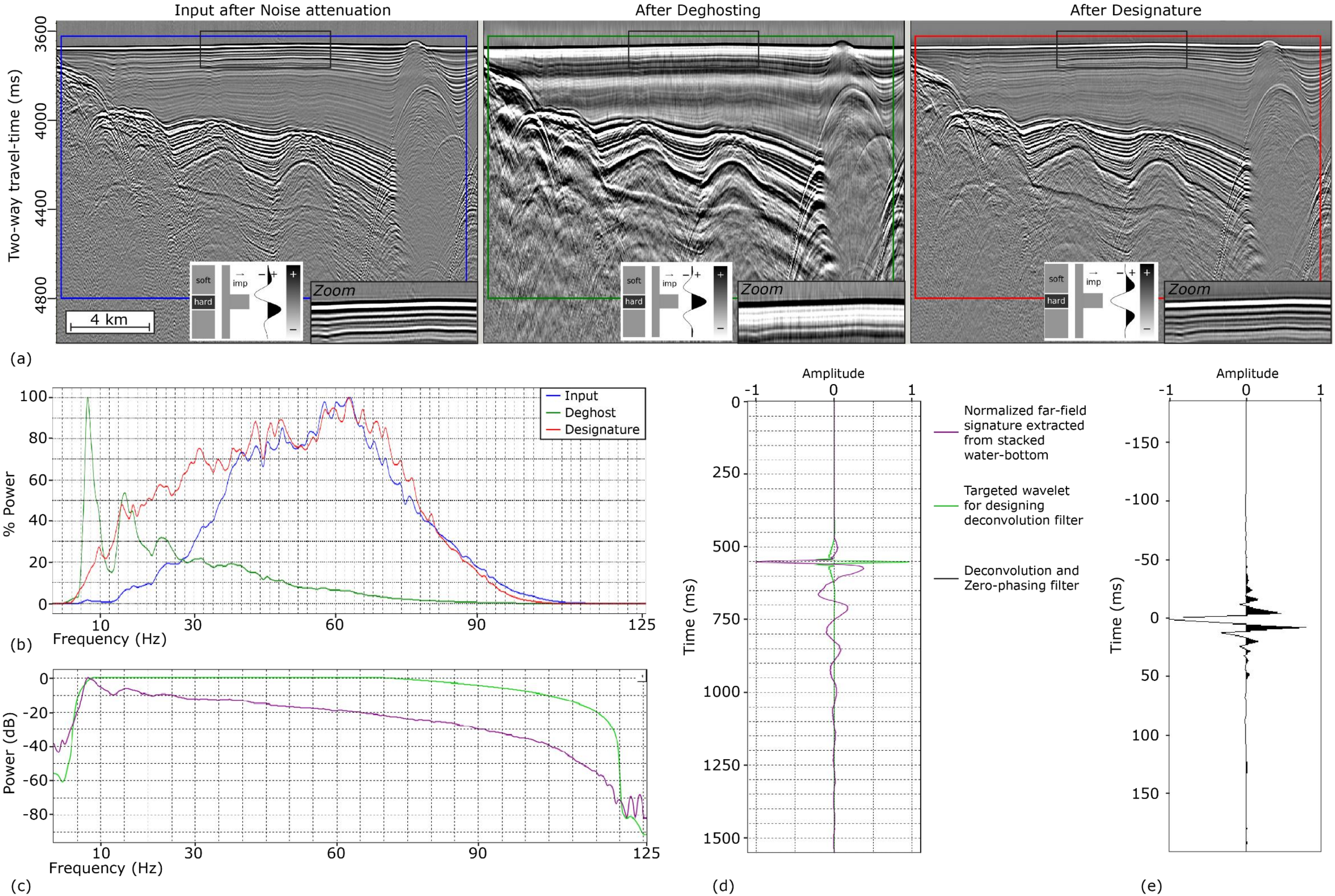

Input after Noise attenuation
After Deghosting
After Designature
Two-way travel-time (ms)
3600
4000
4400
4800
4 km
soft
hard
imp
Zoom
(a)
Input
Deghost
Designature
% Power
Frequency (Hz)
(b)
Power (dB)
Frequency (Hz)
(c)
Amplitude
Time (ms)
Normalized far-field signature extracted from stacked water-bottom
Targeted wavelet for designing deconvolution filter
Deconvolution and Zero-phasing filter
(d)
Amplitude
Time (ms)
(e)

Figure 4 Results from the bandwidth enhancement stage. (a) Near-trace gather before deghosting (left), after deghosting (middle) and after source designature (right); (b) Frequency spectra corresponding to (a); (c) Far-field source signatures estimated from the stacked seabed, overlain with the target Ormsby wavelet used for designing the source designature (debubble and zero-phasing) operator.; (e) The resulting source designature operator

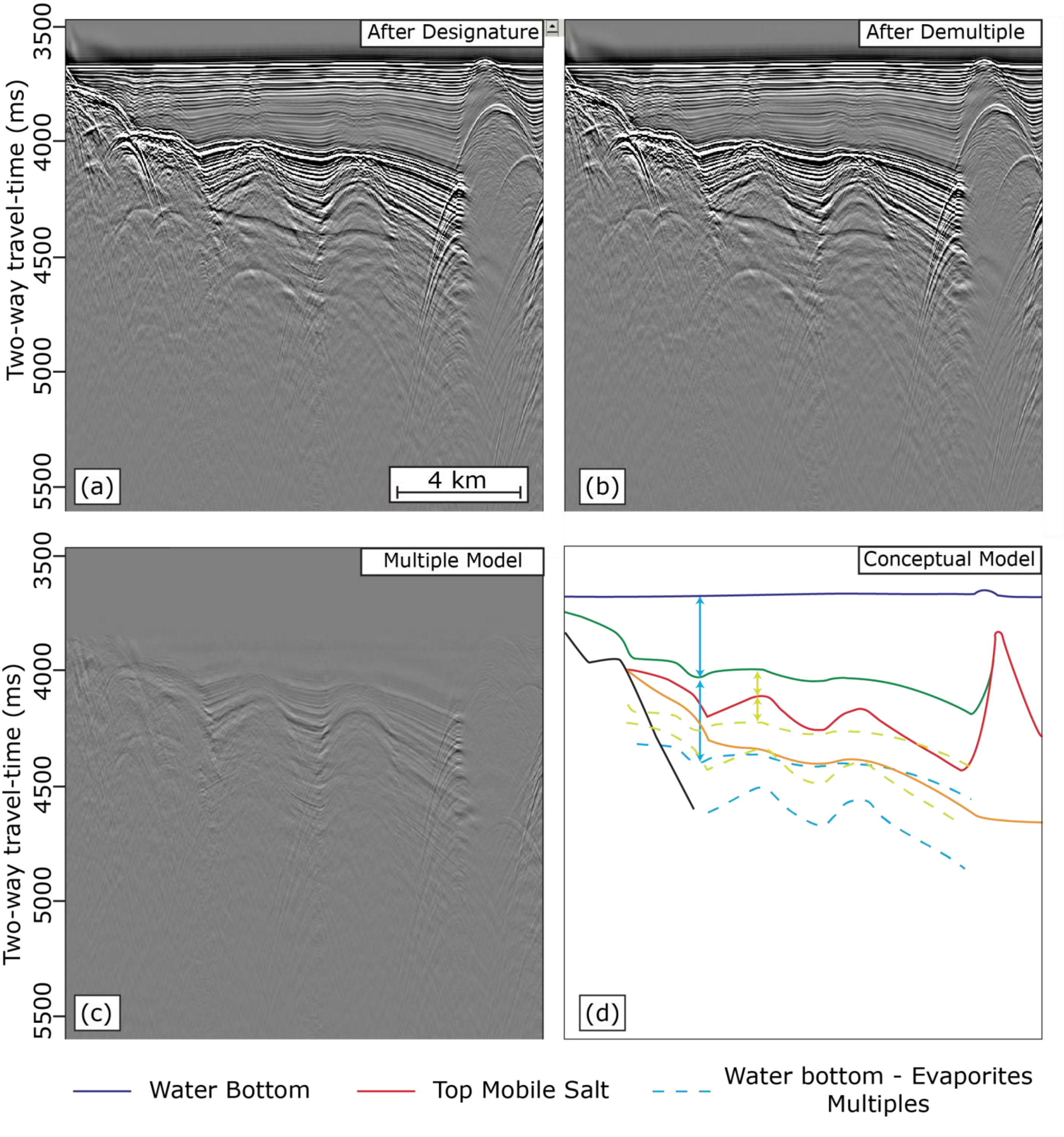

Figure 5 Stacked sections after Radon demultiple. (a) Input data; (b) Demultipled data; (c) Difference between (a) and (b), i.e., the modelled multiples; (d) Sketch cartoon of the major multiple generating horizons and corresponding multiples. Due to the water depth water-bottom (blue) related multiples are not superimposed on the primary reflections in the target geology and are not an issue for the deep-water Algerian basin. Most multiples are observed below the Top Evaporites (green).

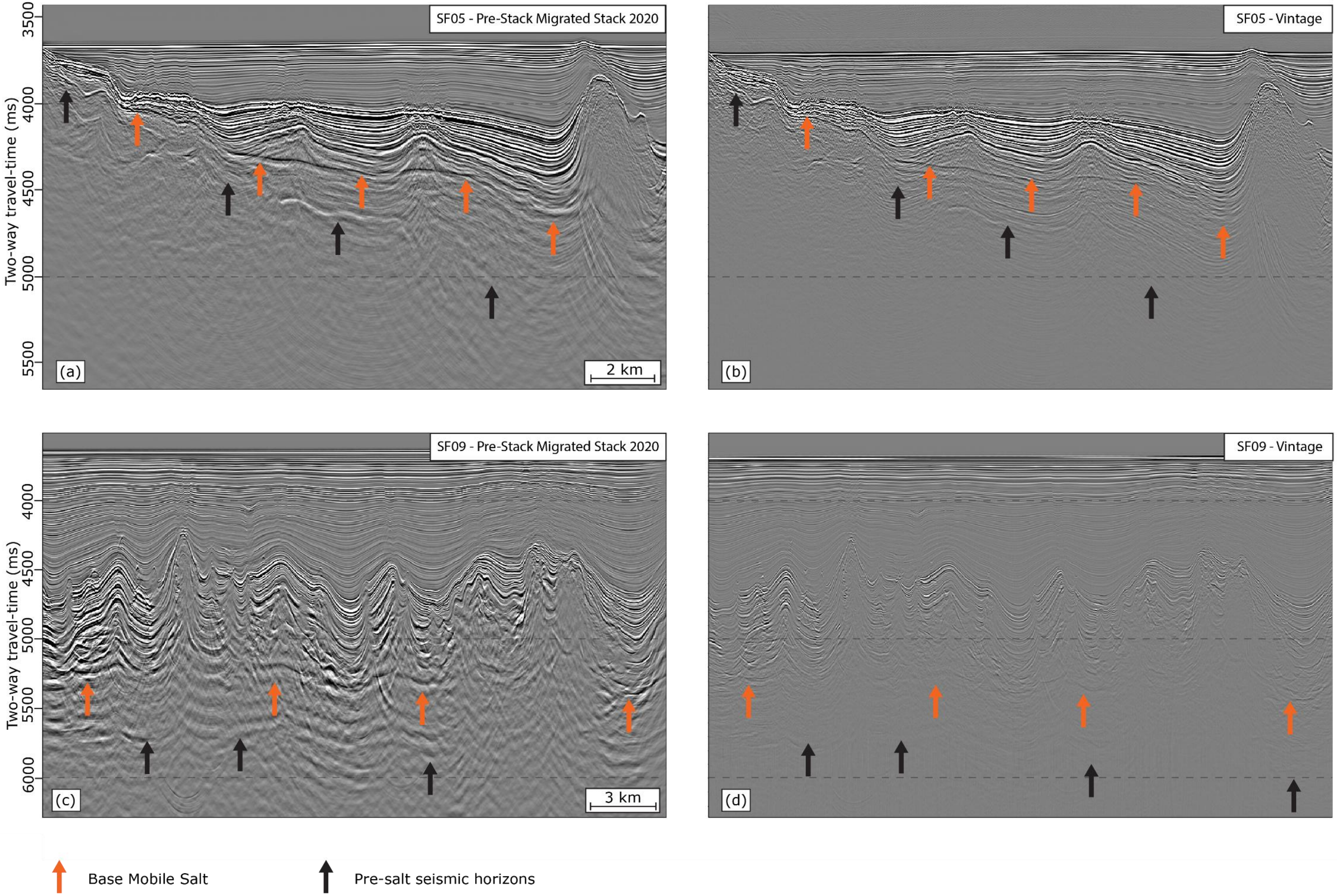
SF05 - Pre-Stack Migrated Stack 2020
SF05 - Vintage
SF09 - Pre-Stack Migrated Stack 2020
SF09 - Vintage
Two-way travel-time (ms)
3500
4000
4500
5000
5500
6000
(a)
(b)
(c)
(d)
2 km
3 km
Base Mobile Salt
Pre-salt seismic horizons

Figure 6 Comparison between the newly re-processed sections (left; a and c) and the vintage sections (right; b and d) in time domain, for sections of lines SF05 (a and b) and SF09 (c and d). Bandwidth enhancement and Radon demultiple allow better imaging of the base salt horizon (orange arrows) and pre-salt horizons (black arrows).

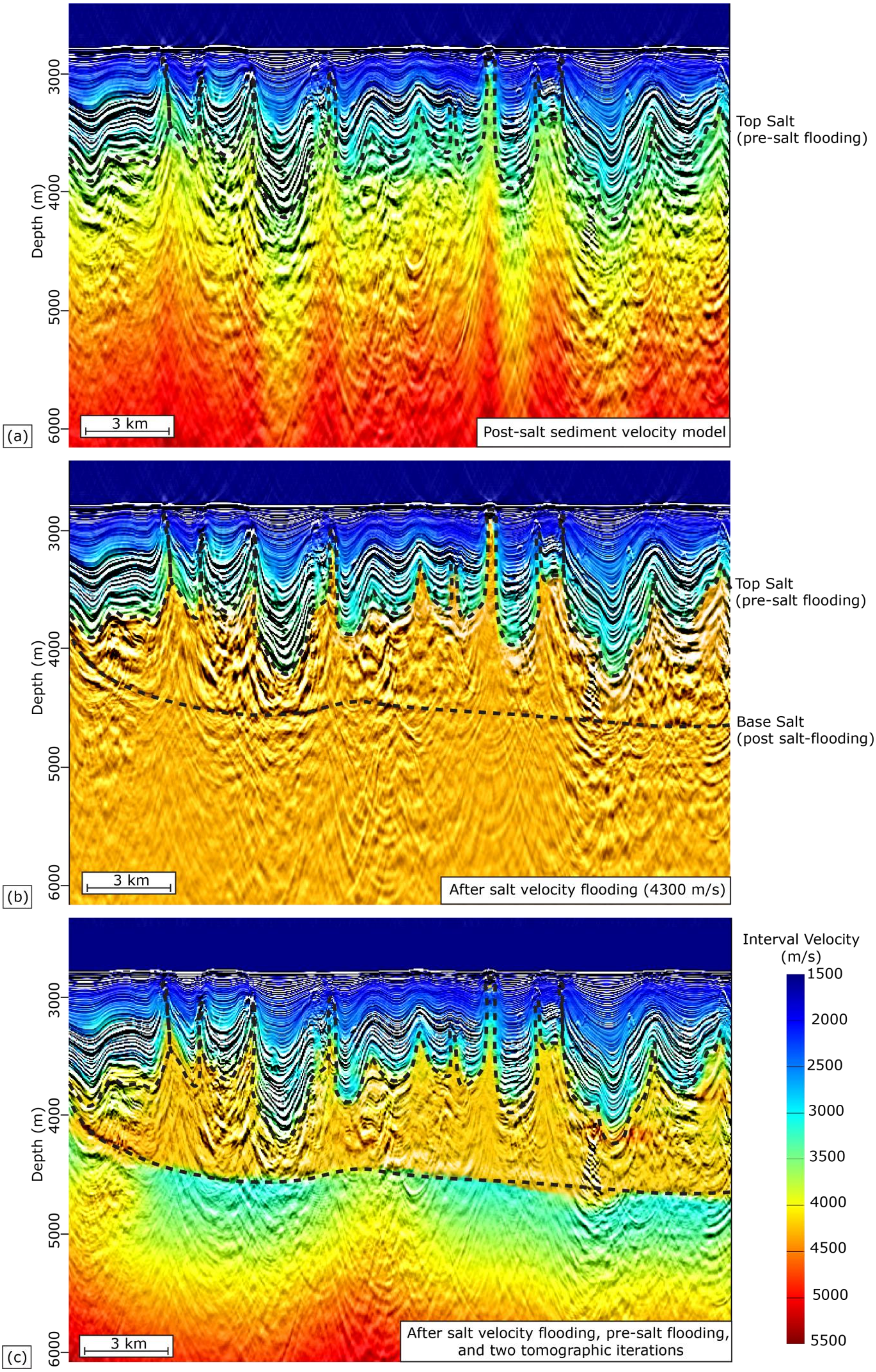

Depth (m)
3000
4000
5000
6000
Top Salt
(pre-salt flooding)
3 km
(a)
Post-salt sediment velocity model
Top Salt
(pre-salt flooding)
Base Salt
(post salt-flooding)
(b)
After salt velocity flooding (4300 m/s)
(c)
After salt velocity flooding, pre-salt flooding,
and two tomographic iterations
Interval Velocity
(m/s)
1500
2000
2500
3000
3500
4000
4500
5000
5500

Figure 7 Pre-stack depth migration sections and velocity models after 3 iteration of tomographic velocity updates in the post-salt (before salt velocity flooding) (a); after salt velocity flooding until the bottom of the sections in order to pick the base salt horizon (b); and after salt velocity flooding between top and base salt horizons and two iterations of tomographic velocity updates post flooding (c).

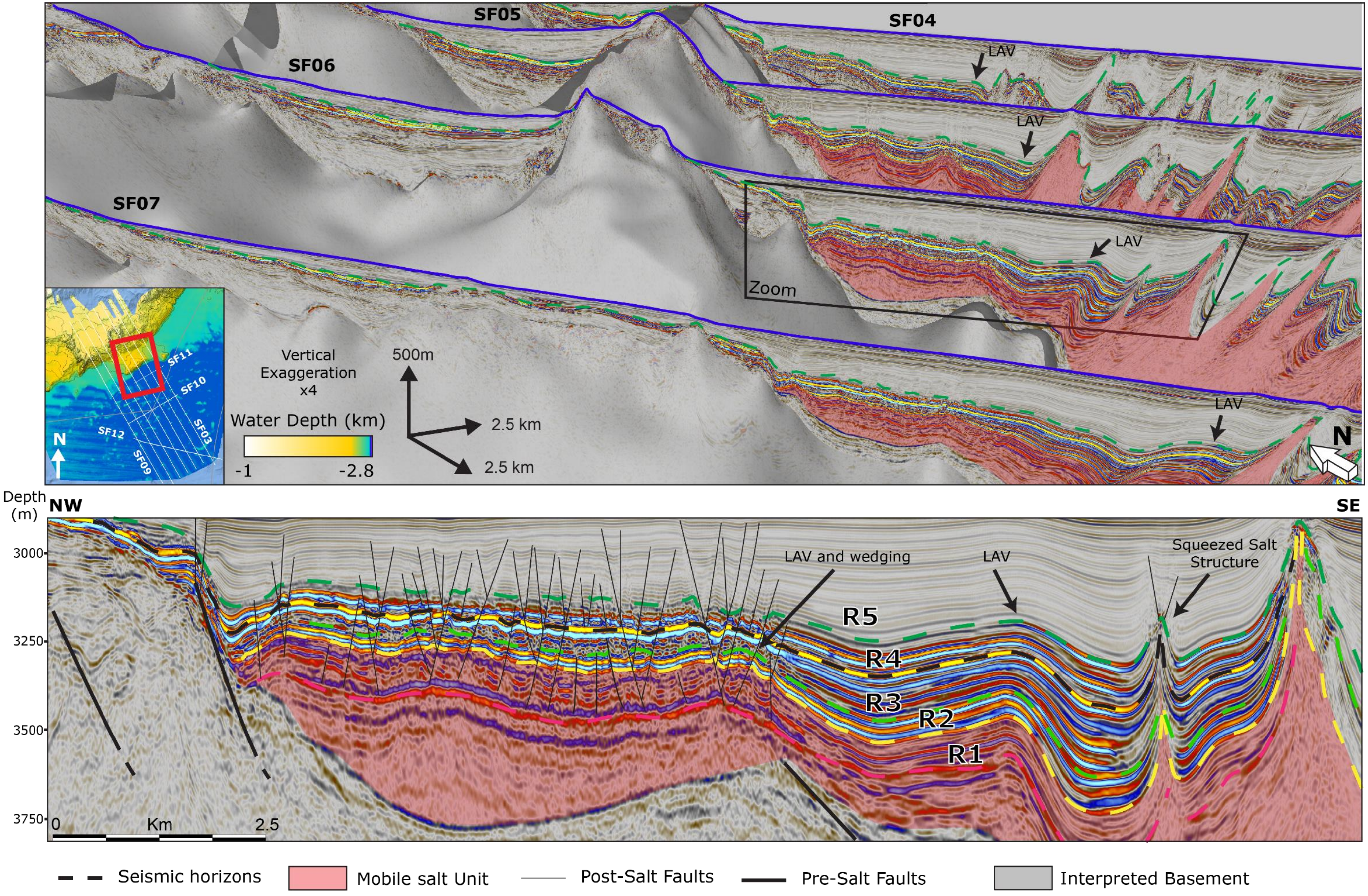

SF05
SF04
SF06
SF07
LAV
Zoom
Vertical Exaggeration x4
500m
2.5 km
2.5 km
Water Depth (km)
-1
-2.8
N
SF11
SF10
SF12
SF03
SF09
Depth (m)
NW
SE
3000
3250
3500
3750
0
Km
2.5
LAV and wedging
Squeezed Salt Structure
R5
R4
R3
R2
R1
Seismic horizons
Mobile salt Unit
Post-Salt Faults
Pre-Salt Faults
Interpreted Basement

Figure 8 3D view of the SALTFLU seismic profiles along the Balearic margin of the Algerian basin, with a zoomed section along line SF06 showing the post-salt Messinian seismic facies. R1, R2, R3 and R4 represents the four seismic horizons observed regionally in the Algerian basin within the evaporites. Vertical exaggeration x5. Positioning map from Figure 1.

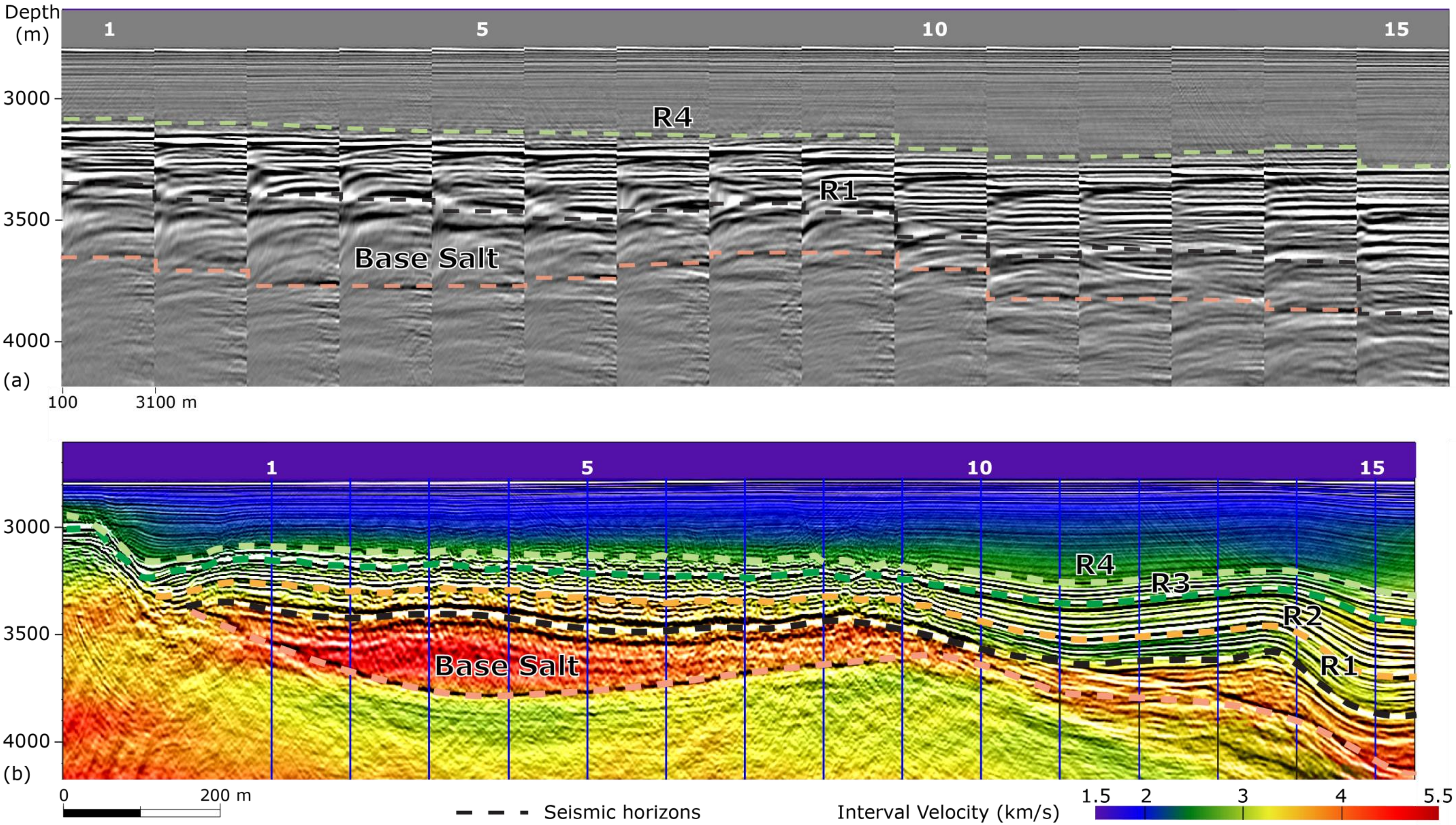

Figure 9 A section of line SF06 after pre-stack depth migration: (a) common reflection-point gathers with interval velocity overlay; (b) a single migrated offset plane (offset 1063 m) with interval velocity overlay (positions of gathers in (a) marked). The velocity of the upper evaporites increases downward from 2500 to 3500 m/s. The mobile salt unit was flooded with 4200 m/s. Two rounds of tomographic velocity updates were performed in the pre-salt sediments after salt velocity flooding.

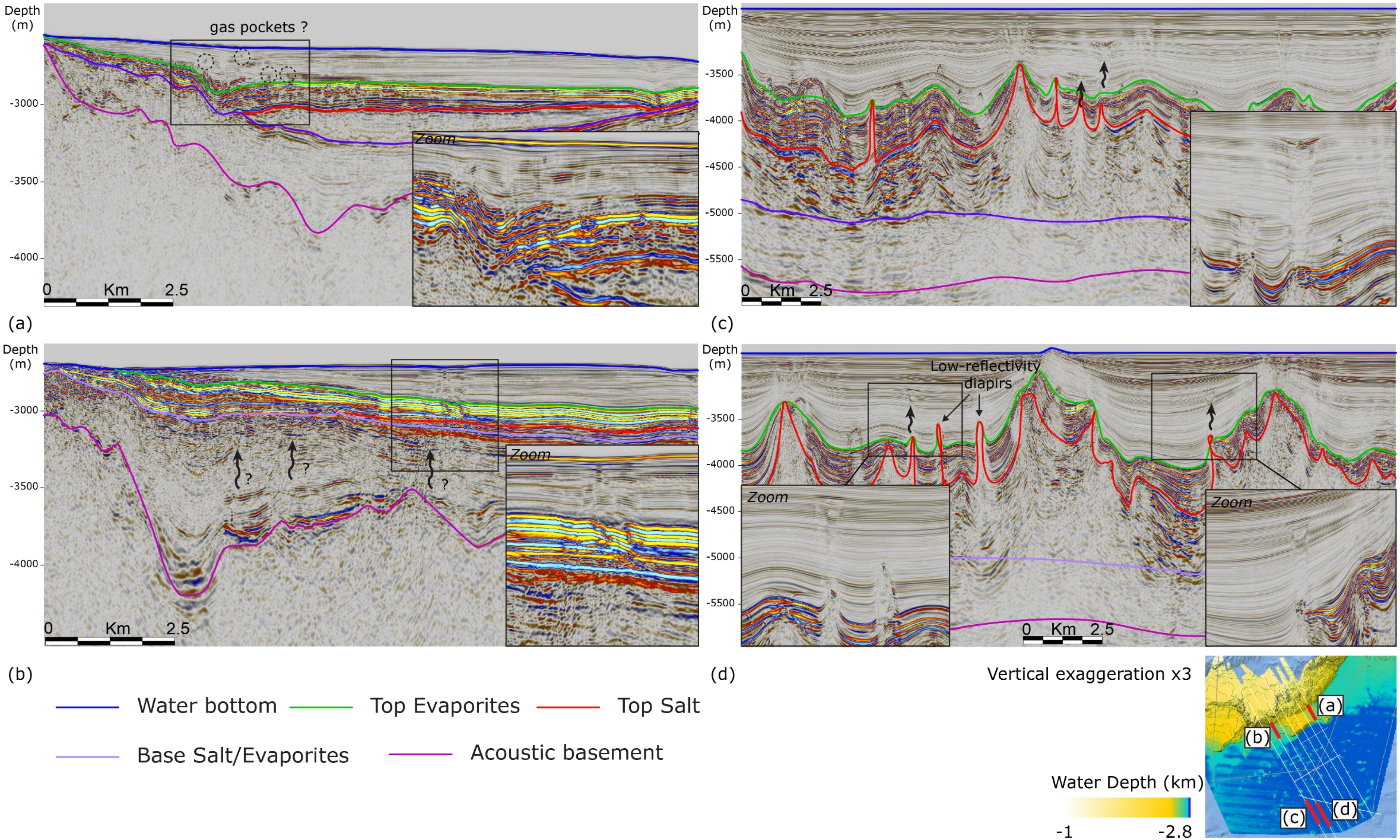

Figure 10 Sections in depth of lines SF03 (a), SF08 (b and d), and SF09 showing amplitude anomalies and disturbed bedding that may indicate the presence of fluid migration. Arrows indicate areas of blanking and/or disturbed bedding, representing possible fluid migration pathways. Vertical exaggeration x3. Positioning map from Figure 1.

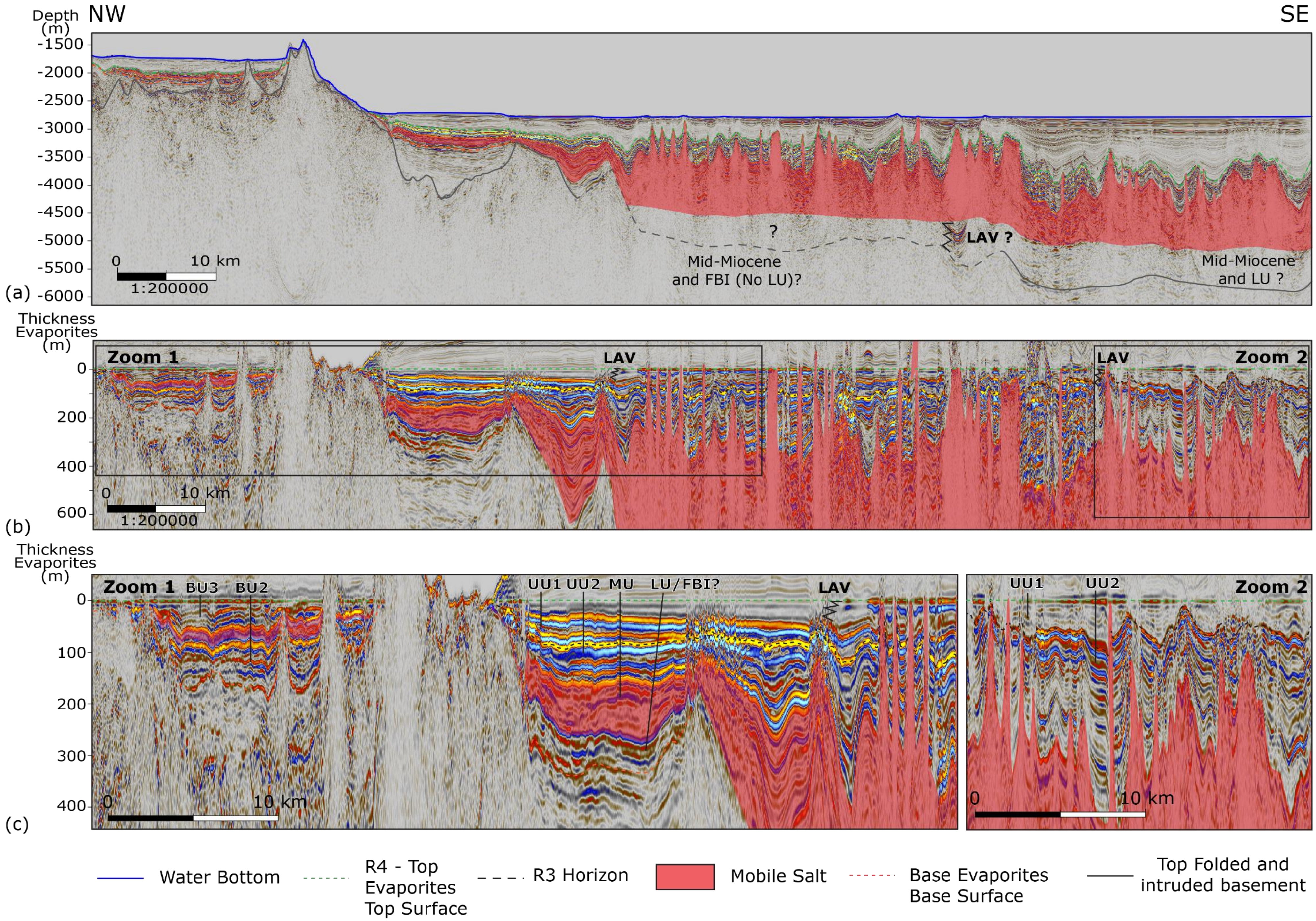

Depth (m)
NW
SE
-1500
-2000
-2500
-3000
-3500
-4000
-4500
-5000
-5500
-6000
(a)
0
10 km
1:200000
?
LAV ?
Mid-Miocene and FBI (No LU)?
Mid-Miocene and LU ?
Thickness Evaporites (m)
Zoom 1
LAV
LAV
Zoom 2
0
200
400
600
(b)
0
10 km
1:200000
Thickness Evaporites (m)
Zoom 1
BU3
BU2
UU1
UU2
MU
LU/FBI?
LAV
UU1
UU2
Zoom 2
0
100
200
300
400
(c)
0
10 km
0
10 km
Water Bottom
R4 - Top Evaporites Top Surface
R3 Horizon
Mobile Salt
Base Evaporites Base Surface
Top Folded and intruded basement

Figure 11 Pre-stack depth migrated line SF09 before (a) and after flattening (b) along seismic horizon R5 (interpreted as the top of the Messinian evaporitic sequence). The two zoomed sections (c) along the flattened line illustrate the comparison between the Bedded Units of the Balearic promontory with the units of the Algerian basin, and the variation in seismic facies within the Messinian Upper Unit in the Algerian basin. Vertical exaggeration x8 for the original line, x20 for the flattened line.

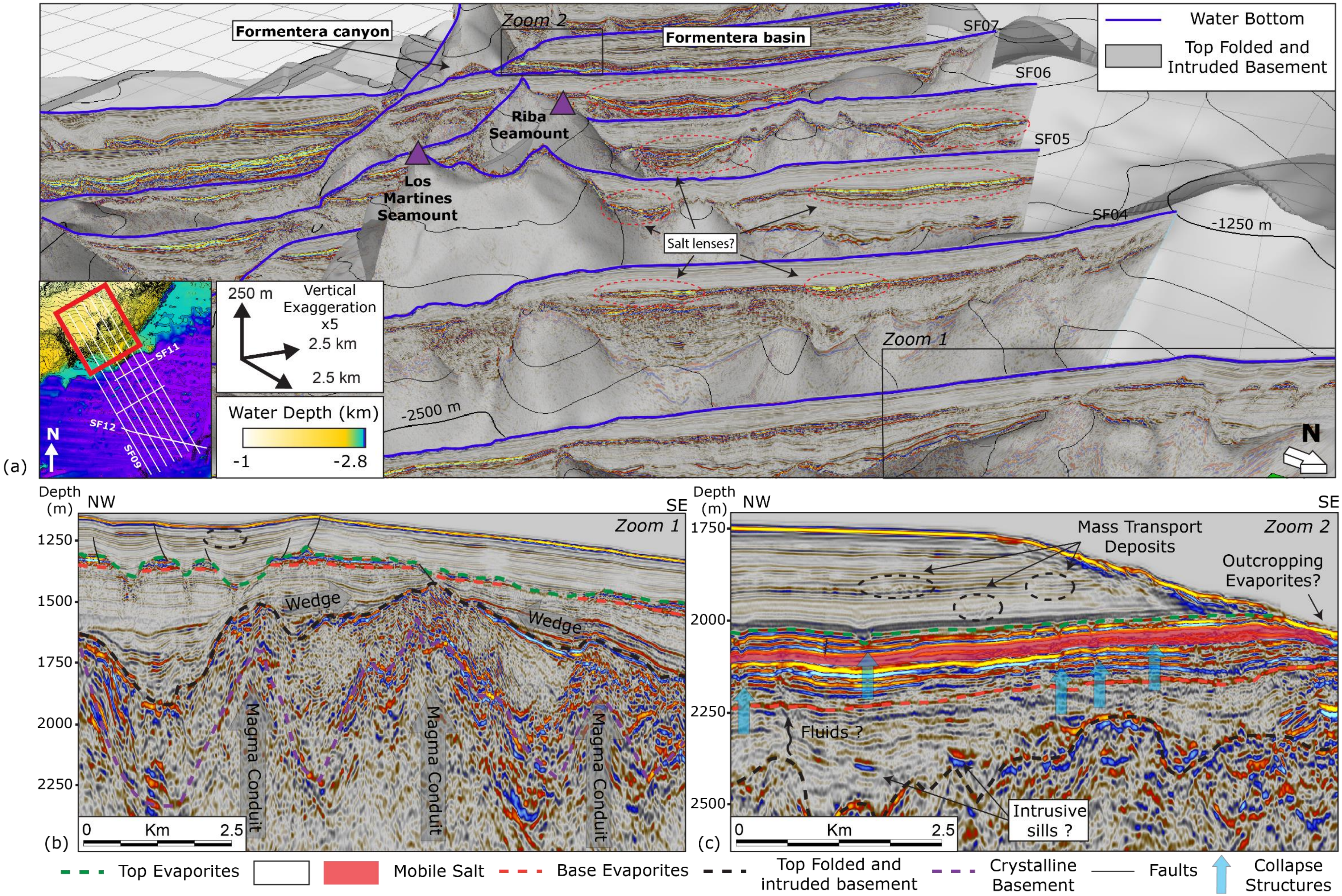

Water Bottom
Top Folded and Intruded Basement
Formentera canyon
Zoom 2
Formentera basin
SF07
SF06
SF05
SF04
Riba Seamount
Los Martines Seamount
Salt lenses?
-1250 m
-2500 m
Zoom 1
250 m
Vertical Exaggeration x5
2.5 km
2.5 km
Water Depth (km)
-1
-2.8
SF11
SF12
SF09
N
(a)
Depth (m)
NW
SE
Zoom 1
Wedge
Wedge
Magma Conduit
Magma Conduit
Magma Conduit
0
Km
2.5
(b)
Zoom 2
Mass Transport Deposits
Outcropping Evaporites?
Fluids ?
Intrusive sills ?
(c)
Top Evaporites
Mobile Salt
Base Evaporites
Top Folded and intruded basement
Crystalline Basement
Faults
Collapse Structures

Figure 12 3-D view of the SALTFLU seismic profiles along the Balearic promontory. Zoom 1 along line SF03 (zoom 1) shows the eroded and incised Messinian evaporites and the underlying volcanic basement, with onlapping wedges at both sides of the volcano. Zoom 2 along line SF08 shows the Messinian evaporites in the Formentera sub-basin, with several depressions at its top that suggest the presence of collapse structures, chaotic seismic facies in the Plio-Quaternary that suggests the presence of mass transport deposits, and disturbed signal below the Evaporites that could indicate fluid circulation. Vertical exaggeration x5

Appendix 1 Impulse response of the Kirchhoff Pre-Stack time migration in the deep Algerian basin, without (a) and with an angle aperture (b)

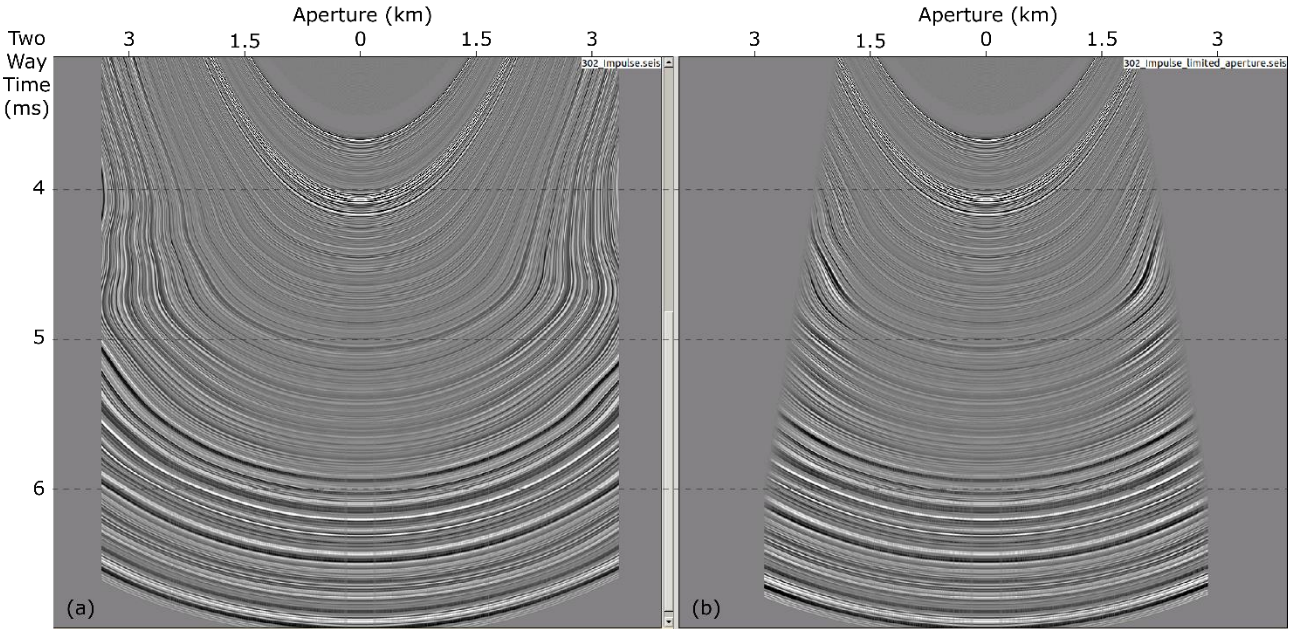

Appendix 2 List of the parameters used for the Kirchhoff pre-stack depth migration

PSDM Parameters	
Ray Tracing	
Gridding	2 CMP x 5meters
Number of rat takeoff angles	25
Maximum takeoff angle	60°
Stepper type	adaptive
Error tolerance	0.0004 m
Mimimum step	4 ms
Maximum step	10 ms
Wavefront step	10 ms
Coincident ray selection	minimum traveltime
Maximum ray separation	100 m
Maximum ray normal divergence	10°
Interpolate rays using	wavefront reconstruction
Maximum ray angle to vertical	90
Maximum travel time	3500 ms
Maximum ray generation	7
Maximum shot time	120 s
Gaps filling	Fast sweeping method for eikonal equations
Kirchhoff prestack depth migration	
Depth increment	5 m
Aperture (Depth/Radius)	1000-1500 /3250-3100/4500-4000
Angle limit to aperture	70°
Trace interpolation factor	8
CMP bin patch size	3
Antialisaing filter increment	2.5 Hz
Antialisaing filter roll-off	20 db/octave
Pad Fast Fourrier Transform	500 samples
Amplitude scaling	2D
Derivative filter	2D

Appendix 3 Depth imaging flow and list of the parameters used for the different tomographic inversion and velocity updates during the velocity model building

Iteration 1 and 2	
L-Matrix Building	
CMP griding	every 2 CMP (12.5m)
Depth griding	5 m, from 0 to 5 km
Raytracing options	
surface tolerance	50 m
stepper type	adaptive
error tolerance	0.0004 m
mimimum step	4 ms
maximum step	10 ms
maximum traveltime	3.5 s
number of ray pairs traced per event	20
Max takeoff angle	50°
Inversion options	
Stopping criterion solver	1%
Maximum number of iterartions	200
Smoothing preconditionner	500m (x) x 10 m (y)
Mask	Seabed to Top Evaporites
Maximum update	-10% to +15%
Laplacian Regularisation	2500 at top, 6000 at bottom

Evaporites Flooding

From top evaporites to bottom line

2500+0.6(\|z-z0\|) m/s

Iteration 3 and 4	
L-Matrix Building	
CMP griding	every 2 CMP (12.5m)
Depth griding	5 m, from 0 to 7 km
Raytracing options	
surface tolerance	50 m
stepper type	adaptive
error tolerance	0.0004 m
mimimum step	4 ms
maximum step	10 ms
maximum traveltime	3.5 s
number of ray pairs traced per event	20
Max takeoff angle	50°
Inversion options	
Stopping criterion solver	1%
Maximum number of iterartions	200
Smoothing preconditionner	1250 (x) x 50 m (y)
Mask	Seabed to Top Salt
Maximum update	-10% to +15%
Laplacian Regularisation	5000 at top, 8000 at bottom

Salt Flooding

4300 m/s, First from Top salt to Bottom line to pick the base salt

Secondly from Top to Base salt

Pre-salt Flooding

2700+1.2(\|z-z0\|) m/s

From Base Salt to Basement or Bottom line (when no basement visible)

Iteration 5 and 6	
L-Matrix Building	
CMP griding	every 2 CMP (12.5m)
Depth griding	5 m, from 0 to 7 km
Raytracing options	
surface tolerance	50 m
stepper type	adaptive
error tolerance	0.0004 m
mimimum step	4 ms
maximum step	10 ms
maximum traveltime	3.5 s
number of ray pairs traced per event	20
Max takeoff angle	50°
Inversion options	
Stopping criterion solver	1%
Maximum number of iterartions	200
Smoothing preconditionner	1500m (x) x 50 m (y)
Mask	Seabed to bottom line
Maximum update	-5% to +15%
Laplacian Regularisation	5000 at top, 8000 at bottom